Journal of Engineering and Technology for Industrial Applications

ISSN ONLINE: 2447-0228

ITEGAM-JETIA

Manaus, v.12 n.58, p.970-980. March/April, 2026.
DOI: https://doi.org/10.5935/jetia.v12i58.3223

RESEARCH ARTICLE OPEN ACCESS

MULTI-OBJECTIVE PELICAN OPTIMIZATION ALGORITHM FOR OPTIMAL PLACEMENT OF EVCSS AND DGS IN RADIAL DISTRIBUTION NETWORKS

Swetha Veligaram*[1], Dr. A Lakshmi Devi[2]

[1 2]Department of EEE, Sri Venkateswara University College of Engineering, Tirupati, Indiamano

[1]https://orcid.org/0009-0008-8294-5580, [2]https://orcid.org/0000-0003-3390-1772

Email: *veligaramswetha@gmail.com, energylak123@yahoo.com

ARTICLE INFO

Article History
Received: January 2, 2026
Reviewed: February 3, 2026
Accepted: March 10, 2026
Published: April 30, 2026

Keywords:
Electric Vehicle Charging Station (EVCS),
Distributed Generators (DG),
Particle Swarm optimization (PSO),
Pelican Optimization Algorithm (POA).

ABSTRACT

The rapid adoption of electric vehicles poses considerable challenges for the operation of radial distribution networks, due to the increased burden and voltage issues at electric vehicle charging stations (EVCS). This paper introduces the Pelican optimization algorithm (POA) for the optimization of distributed generators (DG) to alleviate the negative effects of EVCS loading on the distribution system. Five cases of DG are examined: Type-I (unity power factor), Type-II (reactive power only), Type-IIIA (power factor of 0.85), Type-IIIB (power factor of 0.9), and Type-IIIC (optimized power factor). The proposed methodology is validated by implementing it on two test systems, and the obtained POA results are compared with Particle Swarm Optimization (PSO) results. Type-IIIC DG provides the best overall performance, achieving an impressive 90.39% loss reduction for the IEEE-33-bus system and a remarkable 98.02% reduction for the 69-bus system, and also ensures excellent voltage stability. Type-II DG shows poor performance and is considered unsuitable for practical applications. POA has shown strong effectiveness in achieving the desired objectives, especially with multi-DG configurations

I. INTRODUCTION

The current electric power distribution system is grappling with significant challenges due to rising energy demands, environmental issues, and the need for improved system reliability. Traditional centralized power generation paradigms are gradually expanded by distributed generation (DG) technologies, which offer promising solutions to these complex challenges. Sustainable, economical, and dependable Distributed generation, characterized by small-scale power generation sources located near consumption points, has emerged as a pivotal component in modern power system architecture. These systems reduce power losses in addition to enhancing voltage profiles and improving overall system stability.

Electrification of the transportation sector is increasing worldwide. This transition, while environmentally beneficial, introduces an additional load on existing distribution networks. Electric vehicle charging stations (EVCS) represent a new category of load that is both substantial in magnitude and variable in nature. The higher penetration of EVs into the grid results in increased loads, higher energy losses, and worse voltage profiles. The authors in [1] discuss the impact of EVs on distribution systems, including the volatility of loads, peak demand, and strategies that transform challenges into grid support through real-time management.

The researchers in [2] review optimization techniques applied to EV planning in distribution networks, considering diverse objective functions and load models, including conventional, heuristic, and metaheuristic methods. Integrating distributed generators (DG) is emerging as one of the most effective strategies to address surging global electricity demand. Studies on optimal placement and sizing of DG have consistently shown its effectiveness in significantly enhancing voltage stability, reducing losses, and improving reliability of distribution systems. Reference [3] provides an extensive analysis of optimization frameworks for distribution systems integrating EV charging stations, in conjunction with renewable energy sources, energy storage systems, and distributed generation.

The simultaneous optimization of multiple DG units and EVCS locations transforms this into a complex, multi-objective optimization problem with numerous decision variables and constraints.The majority of the research demonstrates the effectiveness of metaheuristic optimization techniques[4] such as Particle Swarm Optimization (PSO), Genetic Algorithm (GA), Differential Evolution (DE), Ant Colony Optimization (ACO), and various hybrid approaches in addressing the highly non-linear and constrained nature of EV charging station planning problems.

Nevertheless, ongoing research continues to focus on the development of advanced optimization algorithms capable of more efficiently solving the integrated planning challenges associated with EV charging stations and distributed generation. In this context, the present study adopts a novel metaheuristic algorithm, namely the Pelican Optimization Algorithm (POA), to simultaneously optimize the placement and sizing of EV charging stations and distributed generators. Furthermore, different types of distributed generators [5]are considered to effectively mitigate the technical impacts of EV charging integration on distribution network performance.

This paper aims to optimize various types of multiple DGS with EVCS, considering two test systems: IEEE-33 and IEEE-69. A multi-objective function that minimizes active power losses, minimizes the average voltage deviation index (AVDI), and enhances the voltage stability index (VSI) is considered. Minimization of power losses directly impacts operational costs and system efficiency, making their reduction a primary economic objective. The AVDI ensures that voltage levels remain within acceptable bounds throughout the distribution system [6]. The VSI provides crucial information regarding the system's margin to voltage instability, thereby serving as a reliable indicator.

II. PROBLEM FORMULATION

II.1 OBJECTIVE FUNCTION AND ITS CONSTRAINTS

The objective function of the paper is to minimize power loss, AVDI, and enhance VSI.

II.1.1 Active Power Loss:

EVCSs impose substantial load demands, thereby increasing active power loss when they are placed at optimal nodes within the distribution network. Hence, the aim is to minimize the active power loss and is given as:

$$f_1(k) = \min \sum_{k=1}^{N_{br}} R_j * I_j^2 \quad (1)$$

Where R_j is the jth branch resistance, I_j is the current flowing in the jth branch, j is the branch number, and N_{br} is the total number of branches.

II.1.2 Average Voltage Deviation Index:

A node's voltage deviation index is the difference between the node's actual voltage and the reference voltage (1 p.u.) in a network. The AVDI represents the average VDI across all nodes in the network. A lower value signifies greater voltage stability, and it is given as

$$f_2(k) = \frac{1}{b} \sum_{k=1}^{b} |1 - V_k|^2 \quad (2)$$

Where b is the total number of buses, k is the bus number, and V_k is the voltage at the k^{th} bus,

II.1.3 Voltage Stability Index:

The maximum Voltage Stability Index (VSI) of the distribution system indicates that the bus can maintain its voltage profile within acceptable limits, even under varying loading conditions. It is important to keep the VSI of all buses in the distribution system close to unity to ensure the safe operation of the system, and is given as

$$VSI_{k+1} = |V_k|^4 - 4 * [P_{k+1}X_{j-} Q_{k+1} R_j]^2 - 4 * [P_{k+1}R_{j-} Q_{k+1} X_j] |V_k|^2 \quad (3)$$

Where, VSI_{k+1} represents the VSI of (k+1) th bus,P_{k+1} , Q_{k+1}, denotes the active and reactive powers at the (k+1)th bus, $R_j$and X_j represents the resistance and reactance of the j^{th} branch connecting the k^{th} and $(k + 1)^{th}$ bus. During operation, the voltage level of the entire network must be increased by maximizing the VSI of the bus with the lowest value. In this study, three different objective functions are developed to (i) reduce the real power loss, (ii) minimize the Average Voltage Deviation Index (AVDI), and (iii) enhance the Voltage Stability Index (VSI). This multi-objective optimization problem is formulated using a weighted-sum approach and is expressed as:

$$F(k) = \min [w_1(f_1(k) + w_2(f_2(k) + w_3 \frac{1}{f3(k)} \quad (4)$$

where w1 accounts for 50% of the impact on power losses, w2 represents 20% of the effect on AVDI, and w3 reflects 30% of the influence on VSI.

II.2 OPERATIONAL CONSTRAINTS

II.2.1 Equality Constraints

The active and reactive power supplied by the substation must balance the total active and reactive power demand of the system, including the additional load imposed by EV charging stations.

$$P^{substation} + \sum_{k=1}^{N_{bus}} P_{DG}(K) = \sum_{j=1}^{N_{br}} P_{loss}^{j}(k, k+1) + \sum_{k=1}^{N_{bus}} P_{D,k} + P_{EVCS}^{k} \quad (5)$$

$$Q^{substation} + \sum_{k=1}^{N_{bus}} Q_{DG}(K) = \sum_{j=1}^{N_{br}} Q_{loss}^{j}(k, k+1) + \sum_{k=1}^{N_{bus}} Q_{D,k} + Q_{EVCS}^{k} \quad (6)$$

Where N_{br} represents the number of branches, N_{bus} denotes the number of branches, $P^{substation}$, and $Q^{substation}$ are the real and reactive powers of the electric substation, respectively. $P_{DG}(K)$ and $Q_{DG}(K)$, are the k^{th} bus total real and reactive powers injected by DGs, P_{loss}^{j} and Q_{loss}^{j} represents the real and reactive power loss in the j^{th} branch, $P_{D,k}$ and $Q_{D,k}$ are the active and reactive power demand at the k^{th} bus, P_{EVCS}^{k} is the charging station load at $k^{th,}$

II.2.2Inequality Constraints

Voltage magnitude of each bus should lie between 0.95 and 1.05 p.u.

$$V_{min} \leq V_k \leq V_{max} \quad K=1,2,3, \ldots\ldots N_{bus} \quad (7)$$

The limit of line current is as given below

$$I_j \leq I_j^{max} \quad j=1,2,3\ldots\ldots\ldots N_{br} \quad (8)$$

The injected DG power should lie within certain limits

$$DG_{min} \leq DG_{Sizing} \leq DG_{max} \quad (9)$$

II.3 LOAD FLOW ANALYSIS

By [7] proposed a direct approach for load flow solutions, which yields better results, as conventional load flow studies, such as Gauss-Seidel, Newton-Raphson, and Fast Decoupled load flow methods, are not suitable due to the high R/X ratio of distribution networks. This load flow uses two matrices: bus injection to branch current matrix (BIBC) and bus current to bus voltage matrix (BCBV) matrices to calculate the power loss as explained below. The complex load Si in the distribution network is expressed as,

$$S_{i=} Pi+jQ_i \quad \text{for } i=1, 2\ldots\ldots\ldots, N \quad (10)$$

Where P_i, Qi are the real and the reactive powers at the ith bus, N is the total number of buses and the corresponding current injection is given as,

$$I_i = \left(\frac{Si}{V_i}\right)^* \quad (11)$$

Where I_i, V_i are the currents, and voltages at i^{th} bus, respectively the two formulated matrices, BIBC and BCBV, are interconnected as

$$[\Delta V] = [BIBC]\,[BCBV]\,[I] \quad (12)$$

$$[\Delta V] = [DLF]\,[I] \quad (13)$$

Where DLF is the direct load flow matrix. The iterative procedure is done as below

$$I_i^k = \left(\frac{Si}{v_i^k}\right)^* \quad (14)$$

$$[\Delta V^{k+1}] = [DLF]\,[I^k] \quad (15)$$

$$v^{k+1} = [v_o][\Delta V^{k+1}] \quad (16)$$

The power flow is computed as follows

$$P_{i+1} = P_{i-} P_{Li+1} - R_{Li+1} * \left(\frac{P_i^2 + Q_i^2}{|V_i^2|}\right) \quad (17)$$

$$Q_{i+1} = Q_{i-} Q_{Li+1} - X_{Li+1} * \left(\frac{P_i^2 + Q_i^2}{|V_i^2|}\right) \quad (18)$$

Where P_i and Q_i are the real and reactive powers flowing out of bus i, and P_{Li} and Q_{Li} are the real and reactive load powers at bus i. The resistance and reactance of the line section between buses i and i +1 are denoted by $R_{i,i+1}$, and $X_{i,i+1}$, respectively. The power loss of the line section connecting buses i and i +1 may be computed as:

$$P_{Loss}(i, i+1) = R_{Li+1} * \left(\frac{P_i^2 + Q_i^2}{|V_i^2|}\right) \quad (19)$$

$$Q_{Loss}(i, i+1) = X_{Li+1} * \left(\frac{P_i^2 + Q_i^2}{|V_i^2|}\right) \quad (20)$$

The total loss is calculated as

$$P_{T,Loss} = [BIBC] * P_{Loss}(i, i+1) \quad (21)$$

$$Q_{T,Loss} = [BIBC] * Q_{Loss}(i, i+1) \quad (22)$$

$$P_{Loss} = \sqrt{P_{T,Loss}^2 + Q_{T,Loss}^2} \quad (23)$$

III. OPTIMIZATION ALGORITHMS

III.1 PARTICLE SWARM OPTIMIZATION ALGORITHM (PSO)

Particle Swarm Optimization is a population-based stochastic optimization algorithm that addresses various search and optimization challenges by mimicking the collective intelligence observed in natural swarms such as bird flocks and fish schools. It workson a swarm of N particles in a search space with D dimensions. Each particle is a possible answer to an optimisation problem. Each particle progressively adjusts its position by incorporating its previous velocity vector, its individual optimal position (pbest), and the collective optimal position (gbest) disseminated throughout the swarm [8]. Two fundamental equations govern particle dynamics in PSO. For particle *i,* the velocity and position updates are formulated as:

Velocity Update Equation:

$$V_i^{k+1} = \omega^k \times V_i^{k+1} + C_1 \times rand_1 \times (P_{best,i}^k - X_i^k) + + C_2 \times rand_2 \times (G_{best,i}^k - X_i^k) \quad (24)$$

The inertia weight used is calculated using the equation

$$\omega^k = \omega_{max} - \left(\frac{\omega max - \omega min}{kmax}\right) \times k \quad (25)$$

Position Update Equation:

$$X_i^{k+1} = X_i^k + V_i^{k+1} \text{ for i=1, 2,,,,……,n} \quad (26)$$

Where n represents the number of particles in the search space

Algorithm for PSO:

1. Initialize data, EVCS, and DG numbers.
2. Set the number of iterations and other parameters of PSO along with EVCSs and DG lower and upper bound limits.
3. Initialize the velocities and positions of the particle's population in the swarms.
4. Set the iteration to one.
5. Perform the load flow analysis and evaluate the best particle's index, velocities, position, and power losses.
6. Determine the Global optimum and Local optimum
7. According to Equations (24) and (26), update the velocities and locations. The optimal value is assessed, and the optimal particle index for EVCS and DG is identified
8. Update the Gbest and Pbest of swarms.
9. Repeat steps 6–12, incrementing by 1, until the maximum number of iterations is attained.
10. Print the best solution and end.

III.2 PELICAN OPTIMIZATION ALGORITHM (POA)

The POA is based on the hunting methods of pelicans, which [9]. When pelicans are hunting, they work in groups in search of their prey and then dive strategically, extending their wings to direct the prey towards the water's surface and shallow areas, which makes it easier to catch. It initializes a population of pelicans that change their positions according to the optimal solutions to simulate prey pursuit. The algorithm guarantees global optimization through dynamic exploration of new regions. This leads to stable and efficient solutions for difficult problems. The initialization of the population is done by

$$X_{i,j} = l_j + \text{rand}.(u_j - l_j) \text{ , i=1, 2,……, N, j=1,2….m} \quad (27)$$

Where X_(i,j) denotes the value of the jth variable as defined by the ith candidate solution, lj signifies the jth lower bound, and uj denotes the jth upper limit of the problem variable, rand is a random number in the interval [0, 1], N represents the number of population members, and m indicates the number of problem variables in this POA, the population of pelican agents is represented by a population matrix. Each row corresponds to a candidate solution vector, while each column denotes the recommended values for the decision variables

$$X=\begin{bmatrix} X_1 \\ \vdots \\ X_i \\ \vdots \\ X_N \end{bmatrix}_{N\times m} = \begin{bmatrix} x_{1,1} & \dots & x_{1,j} & \cdots & x_{1,m} \\ \vdots & \vdots & \vdots & \vdots & \vdots \\ x_{i,1} & \dots & x_{i,j} & \dots & x_{i,m} \\ \vdots & \vdots & \vdots & \vdots & \vdots \\ x_{N,1} & \dots & x_{N,j} & \dots & x_{N,m} \end{bmatrix}_{N\times m} \quad (28)$$

Where X is the population matrix, and Xi represents the ith individual pelican. The above initial populations are used to determine the objective functions in the vector form, as shown below

$$F = \begin{bmatrix} F_1 \\ \vdots \\ F_i \\ \vdots \\ F_N \end{bmatrix}_{N\times 1} = \begin{bmatrix} F(X_1) \\ \vdots \\ F(X_i) \\ \vdots \\ F(X_N) \end{bmatrix}_{N\times 1} \quad (29)$$

The POA approach is represented in two phases based on pelicans' hunting behavior. The hunting behavior is simulated using two phases

(i) Moving towards prey

Exploration entails moving toward the prey, whereas exploitation necessitates gliding on the water's surface. During the initial phase, pelicans randomly identify and approach their prey within the search space, mathematically represented by the equation

$$x_{i,j}^{p_1} = \begin{cases} x_{i,j} + rand.(p_j - l.x_{i,j}), & F_p^1 < F_i \\ x_{i,j} + rand.(x_{i,j} - p_j), & else \end{cases} \quad (30)$$

Where Fp represents the prey objective function value. A pelican agent's new position is accepted only if it yields a better objective function value. This effective updating criterion steers the algorithm away from suboptimal regions, avoiding premature convergence to local optima. The position of the POA is updated using the equation below

$$X_i = \begin{cases} X_i^{P_1}, F_i^{P_1} < F_i ; \\ X_i , else , \end{cases} \quad (31)$$

(ii). Winging on the water surface

During this phase, pelicans use the surface of the water to push fish up by spreading their wings, thereby catching the fish in their throat bag. Pelicans capture a greater quantity of fish in the region targeted by this method. During this phase, the algorithm gets closer to finding better solutions in the hunting zone, which makes it easier to take advantage of POA. This pelican's hunting behaviour is written mathematically as

$$x_{i,j}^{p_1} = x_{i,j} + R.\left(1-\frac{t}{T}\right).(2.\,rand - 1).\,x_{i,j} \quad (32)$$

Effective updating has been used to decide whether to accept or reject the most recent pelican position, as shown in the equation below.

$$X_i = \begin{cases} X_i^{P_2}, F_i^{P_2} < F_i ; \\ X_i , else , \end{cases} \quad (33)$$

Algorithm Procedure

1. Initialize the bus and line data, EVCS, and DG numbers.
2. Initialize the number of iterations and other parameters of POA along with EVCSs and DG lower and upper bound limits.
3. Randomly initialise the places of the pelican population inside the defined search space limits for EVCS sites and DG capacity.
4. Set the iteration counter t = 1.
5. Evaluate the fitness of each pelican using load flow analysis and other performance indices for the current EVCS and DG placement configuration.
6. Identify the global best position (x_best) representing the optimal EVCS and DG configuration with minimum power losses.
7. Generate a random prey position within the search space bounds.
8. Update positions using equations (27)-(31)
9. Run load flow analysis for all updated pelican positions to evaluate new fitness values.
10. Update the global best position if any pelican achieves better performance (lower power losses) than the current global best.
11. Check boundary constraints for EVCS locations (valid bus numbers) and DG capacities (within specified limits). Apply corrections if positions violate bounds.
12. Increment iteration counter: t = t + 1 and repeat steps 7-13, till the maximum number of iterations is attained
13. Print the best solution and end.

IV. RESULTS AND DISCUSSIONS

IV.1 SYSTEM DESCRIPTION:

The initial test system is the IEEE-33 bus distribution network, with 33 nodes and 32 branches, with a total real power demand of 3715 kW and total reactive power loads of 2300 kVAr [10]. The second test system is the IEEE-69 bus distribution network, with 69 nodes and 68 branches, with a total real and reactive demand of 3803.9 kW and 2693.1 KVAR. Both systems operate at 100 MVA and 12.66 kV. Table 1 shows the electric vehicle (EV) models that are considered in this paper. These include the BMW i3, Tesla Model X, Chevrolet Volt, and Chang'an Yidong. Charging stations (CS) equipped with AC/DC level-2 charging ports (CPs) compliant with the SAE J1772 standard are also included. These ports are capable of charging both Battery Electric Vehicles (BEVs) and Plug-in Hybrid Electric Vehicles (PHEVs) with a maximum power output of 7 kW[6].

Table 1: EVCS Features for Simulation.

Tesla Model X	13	15	195
BMW i3	44	10	440
Chevrolet Volt	2.2	25	55
Chang An Yidong	3.75	20	75
SAE J1772 Standard	7	30	210
Total CS power rating (kW)		100	975

Source: Authors, (2026).

Three different scenarios are addressed in this work on two IEEE systems to validate the methodology

Scenario 1: Base case

Scenario 2: Optimal placement of three EVCSs

Scenario 3: Optimal placement of three EVCSs with three DGs of different types

IV.2 RESULTS OF THE IEEE-33 BUS SYSTEM

Scenario 1: Base case

With the load flow analysis on the first test system, the base case real power and reactive power losses are 202.66kW and 134.7 kVAr, respectively. The minimum voltage of 0.9131 p.u is obtained at bus 18, whereas the minimum VSI value is 0.6951 p.u, and the AVDI minimum is 0.0036 p.u

Scenario 2: Optimal placement of three EVCSs

When multiple EVCSs of 975 kW are optimally placed with the considered optimization algorithms, system performance improves, rather than random placement. Both PSO and POA identified the optimal locations for three EVCSs as 2,19,25. With the identified locations, the power loss becomes 287.1126 kW, VSI decreased to 0.678644 p.u., and AVDI increased to 0.004313 p.u. This result underscores the importance of optimization of DGS with EVCS in the distribution system.

Table 2: Results of the IEEE-33 bus system with and without EVCSs.

	Locations	**Ploss(kW)**	**AVDI (p.u)**	**VSI (p.u)**	**Vmin (p.u)**
Load Flow					
Base Case	-	202.66	0.00366	0.6951	0.9131
Three EVCSs (3*975kW)					
PSO	2,19,25	287.1126	0.004313	0.678644	0.9076
POA	2,19,25	287.1126	0.004313	0.678644	0.9076

Source: Authors, (2026).

Scenario 3: Optimal placement of three EVCSs with three DGs of different types

In this case, three DGs of different types are optimally placed in conjunction with three EVCS of 975 kw in the radial distribution system. Type-3 DGs with different power factors (0.85, 0.9) and an optimized power factor are considered in this study. With optimization algorithm PSO, the losses for Type-1, Type-2, Type-3A, Type-3B, Type-3C are reduced to 69.22 %,21.19%,87.86%,87.47 % and 89.66 %. The AVDI values have become 0.000459 p.u., 0.001507 p.u., 0.000019 p.u., 0.000031 p.u., and 0.000029 p.u.Also, the VSI values have increased to 0.813721 p.u.,0.873617 p.u., 0.968282 p.u., 0.950191 p.u.,0.957584 p.u., as shown in Table 3.

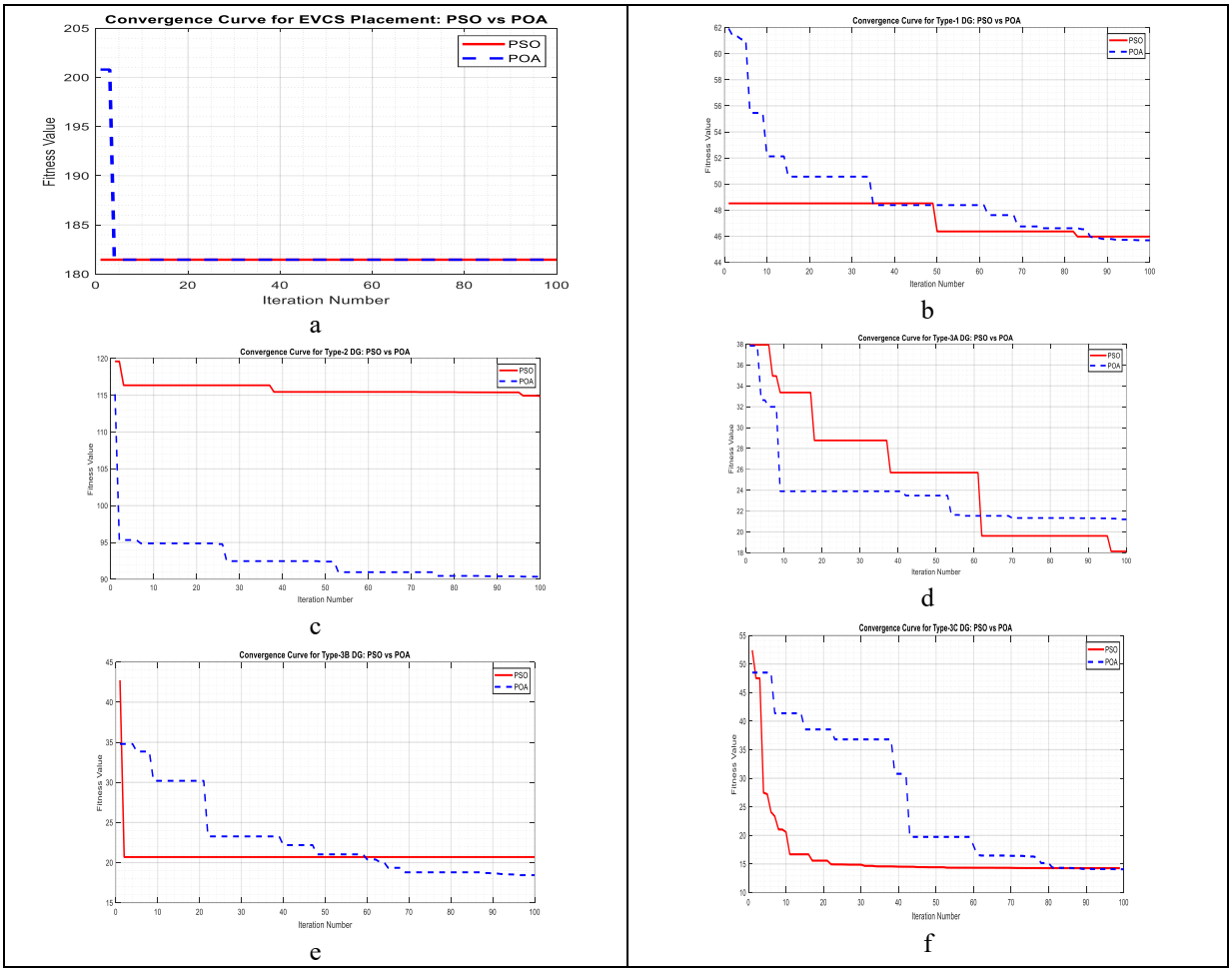

Figure 1: Convergence Curves of the IEEE-33 bus system with optimization algorithm a) With EVCSs only b). EVCSs with Type-1 DGs c). EVCSs with Type-2 DGs d). EVCSs with Type-3A DGs e). EVCSs with Type-3B DGs f). EVCSs with Type-3C DGs. Source: Authors, (2026).

Table 3: Performance Indices of IEEE-33 bus system.

	Locations	**Sizes**	**Ploss (kW)**	**% Reduction in Loss**	**AVDI (p.u)**	**VSImin (p.u)**	**Vmin (p.u)**
Type-1 (kW)							
PSO	29,24,13	1168,2098,754	88.3920	69.22	0.000459	0.873617	0.9668
POA	24,13,30	2178,1083,793	87.7551	69.43	0.000438	0.880739	0.9688
Type-2 (kVAr)							
PSO	10,30,17	468,1295,336	226.2993	21.19	0.001507	0.813721	0.9500
POA	7,16,30	813.16 453.07,1105.75	224.7136	21.74	0.001431	0.814559	0.9500
Type-3A (kVA)							
PSO	30,13,24	1256+i77 728+i451 1904+i1180	34.891	87.86	0.000019	0.968282	0.9920
POA	24,14,30	1739+i1078 735+i455 1216+i75	34.6845	87.92	0.000022	0.967913	0.9919
Type-3B (kVA)							
PSO	11,30,24	951+i461 1260+i610 1885+i913	35.9690	87.47	0.000031	0.950191	0.9873
POA	24,13,30	2006+i971 668+i324 1269+i615	35.2785	87.71	0.000058	0.954793	0.9890
Type-3 C(kVA)							
PSO	24,14,30	2137+550 766+i359 1073+i968.7	29.6863	89.66	0.000029	0.957584	0.9893
POA	24,12,30	2043.64+i356 916.54 +i61 958.61+i902	27.5781	90.40	0.000027	0.965020	0.9915

Source: Authors, (2026).

With POA the losses Type-1, Type-2, Type-3A, Type-3B, Type-3C DGs are reduced to 69.43 %,21.74%,87.92%,87.71 % and 90.40 %. The AVDI values have become 0.000438 p.u., 0.001431 p.u., 0.000022 p.u., 0.0000528 p.u., and 0.000027 p.u.Also, the VSI values have increased to 0.880739 p. u,0. 814559p.u, 0.967913p.u,0.954793 p.u, and 0.965020 respectively.

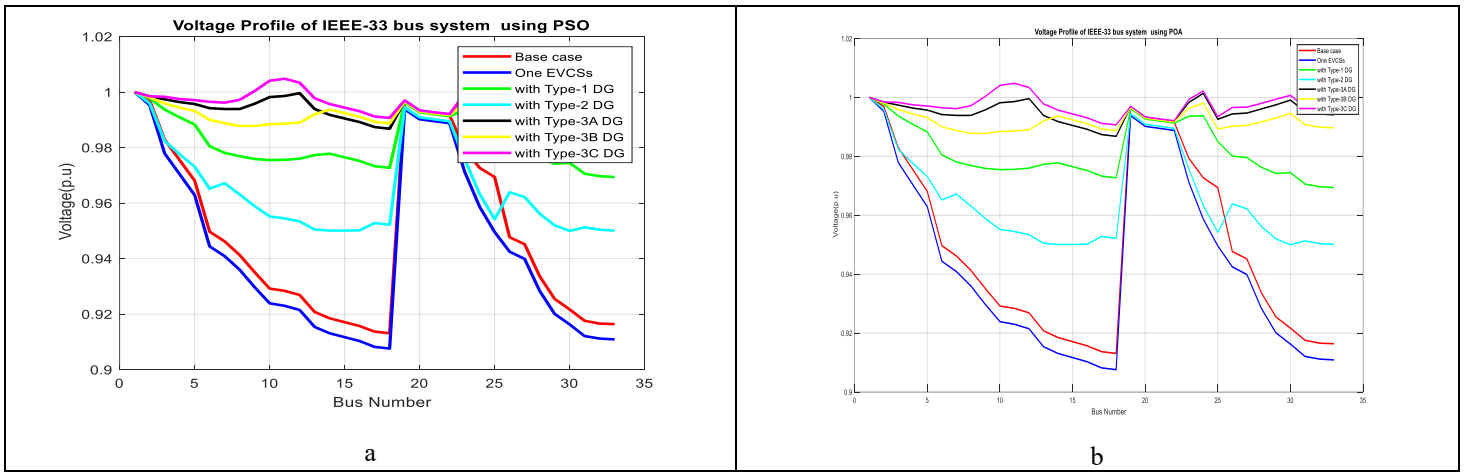

Figure 2: Comparison of the voltage profile within the IEEE-33 bus system, a) with PSO, b) with POA.
Source: Authors, (2026).

The results show that Type-3C with optimal power flow achieves the highest loss reduction, at 89.66% using PSO, followed closely by 90.40% with POA. The minimum voltage is better with POA, which is 0.9915 p.u., as shown in Figure 2. Fig. 1 also shows the convergence curve for three EVCSs with three different types of DGs. The final curves for POA and PSO are similar, but POA converges more smoothly.

IV.3 RESULTS OF THE IEEE-69 BUS SYSTEM

Scenario 1: Base case

With the load flow analysis on the IEEE-69 bus system, the base case real power and reactive power losses are 224.8807kW and 102.64393 kVAr, respectively. The minimum voltage of 0.9092 p.u is obtained at bus 65, whereas the minimum VSI value is 0.683325 p.u, and the AVDI minimum is 0.001460 p.u.

Scenario 2: Optimal placement of three EVCSs

Both the optimization algorithms PSO and POA identified the optimal locations for three EVCS as 2,28, and 47 for the IEEE-69 bus. The power loss increased to 225.2724 kW. Additionally, VSI is decreased to 0.683224 p.u. and AVDI is increased to 0.001462 p.u.

Table 4: IEEE-69 bus system performance before and after placement of EVCS.

	Locations	Ploss(kW)	AVDI(p.u)	VSImin (p.u)	Vmin(p.u)
Load Flow					
Base Case	-	224.8807	0.001460	0.683325	0.9091
Three EVCSs (3*975kW)					
PSO	2,28,47	225.2724	0.001462	0.683244	0.9092
POA	2,28,47	225.2724	0.001462	0.683244	0.9092

Source: Authors, (2026).

Scenario 3: Optimal placement of three EVCSs with Three Different Types of DGS

With the Type-I configuration (3 DGs integrated with 3 EVCS), the system achieved a power loss reduction of 69.10%. The minimum bus voltage improved to 0.9790 p.u. using POA and 0.9789 p.u. using PSO. The voltage stability index increased to 0.918686 p.u. and 0.918304 p.u., while the average voltage deviation index decreased to 0.000076 p.u. and 0.000077 p.u. for POA and PSO optimizations.

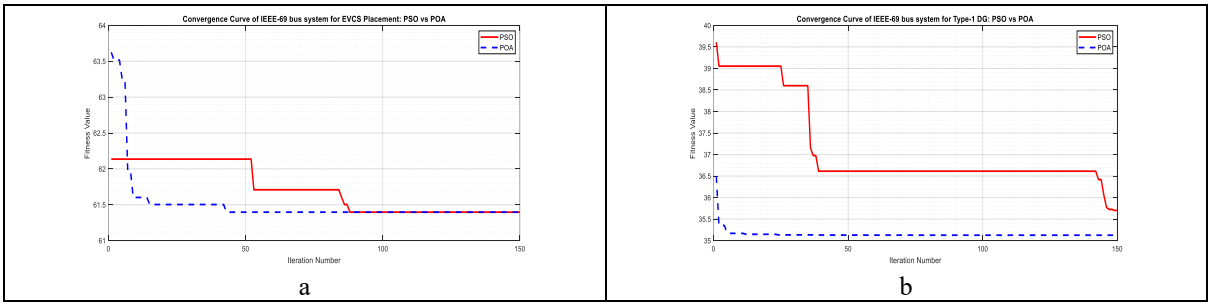

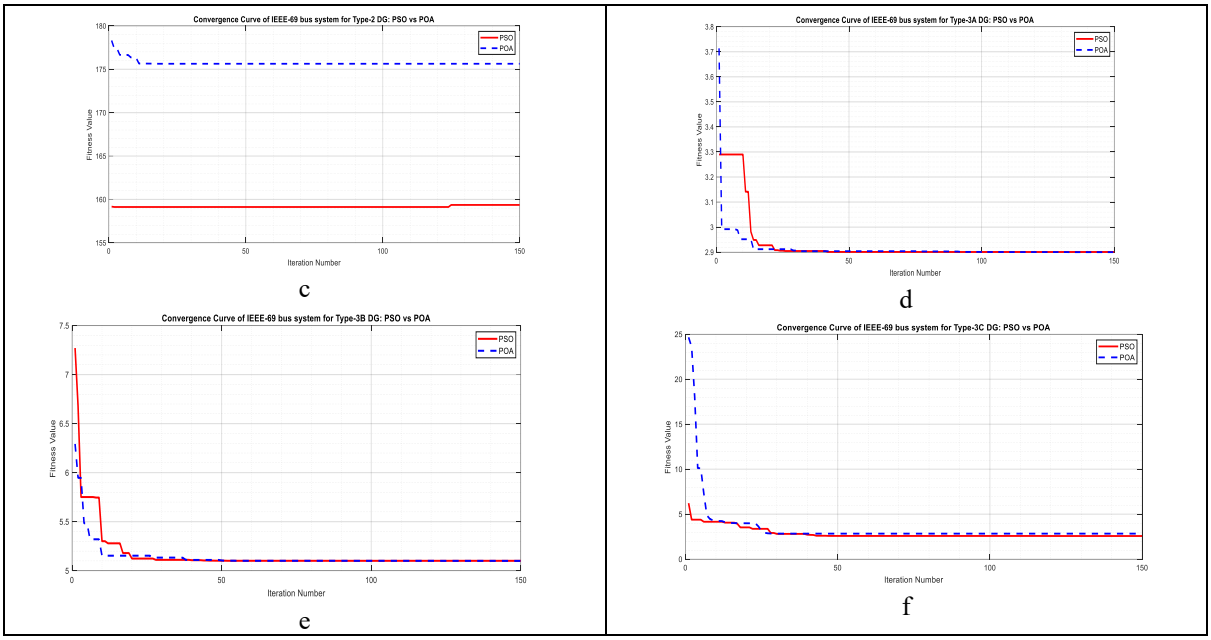

Figure 3: Convergence Curves of the IEEE-33 bus system with optimization algorithm a) With EVCSs only b). EVCSs with Type-1 DGs c). EVCSs with Type-2 DGs d). EVCSs with Type-3A DGs e). EVCSs with Type-3B DGs f). EVCSs with Type-3C DGs. Source: Authors, (2026).

With Type-2 DG, power losses decreased to 155.233kW and 155.22 kW. The voltage stability index (VSI) improved to approximately 0.7497 p.u., while the minimum bus voltage reached 0.9305 p.u. for both methods. The average voltage deviation index (AVDI) was measured at 0.000742 p.u. for both POA and PSO approaches. The results are tabulated in 5.

Table 5: Performance Indices of IEEE-69 bus system.

	Locations	**Sizes**	**Ploss (kW)**	**% Reduction in Loss**	**AVDI (p.u)**	**VSImin(p.u)**	**Vmi (p.u)**
Type-1 (kW)							
PSO	17,11,61	362,578,1712	69.6193	69.09	0.000077	0.918304	0.9789
POA	17,11,61	380,530,1720	69.5989	69.10	0.000076	0.918686	0.9790
Type-2 (kVAr)							
PSO	17,11,61	467,1000,1000	155.233	31.08	0.000742	0.749738	0.9305
POA	18,11,61	466,1000,957	155.22	31.09	0.000742	0.749736	0.9305
Type-3A (kVA)							
PSO	17,11,61	386+i239 517+i320 1746+i1082	5.1876	97.70	0.000002	0.977075	0.9942
POA	11,18,61	519+i32 387+i240 1745+i1082	5.186	97.70	0.000002	0.977075	0.9942
Type-3B (kVA)							
PSO	17,11,61	406+i196 543+i263 1829+i886	9.5878	97.44	0.000002	0.977038	0.9942
POA	11,18,61	544 +i264 405+i196 1829+i886	9.5863	95.74	0.000002	0.977038	0.9942
Type-3C (kVA)							
PSO	17,11,61	380+i251 494+i353 1676+i1195	4.4583	98.02	0.000002	0.977092	0.9942
POA	11,61,18	496+i354 1675+i1195 379+i251	4.4567	98.02	0.000002	0.977092	0.9942

Source: Authors, (2026).

Type-3A (3DGs) reduced power losses to 5.186 kW and 5.1786 kW, VSI increased to 0.977075 p.u, and AVDI decreased 0.000002 p.u, while Vmin reached 0.9942 p.u, for POA and PSO. Type-3B (3DGs) reduced power losses to 9.5878 kW and 9.586 kW, minimum voltage reached 0.9942 p.u, VSI increased to 0.977038 p.u, and AVDI decreased to 0.000002 p.u, for POA and PSO, respectively.

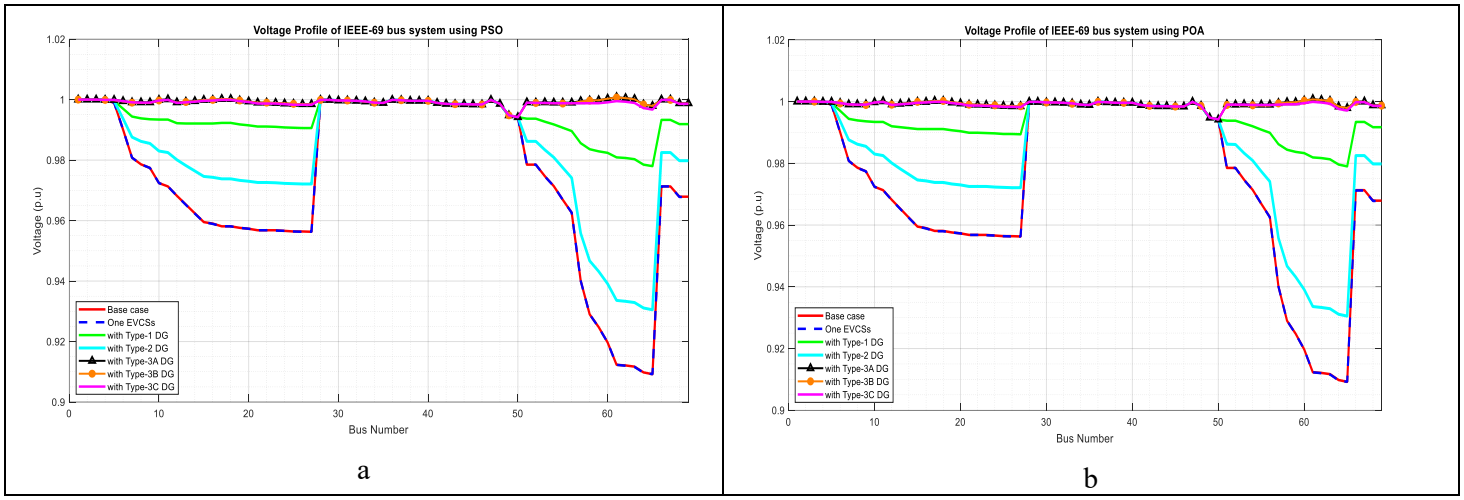

Figure 4: Comparison of the voltage profile within the IEEE-69 bus system, a) with PSO, b) with POA.
Source: Authors, (2026).

For type-3C, DGs with optimized power factors are determined with both optimization algorithms. This reduced power losses to 4.4567 kW and 4.4583 kW, and voltage profiles increased to 0.9942 p.u., VSI increases 0.977092 p.u and AVDI decreases 0.000002 p.u., for POA and PSO, respectively, as shown in Table 5. Type -3 C Dg achieved power loss reduction of 98.02 % with both theoptimization algorithms. The convergence curves shown in Figure 3 prove that the new algorithm, POA, outperforms the PSO in fitness value. Figure 4 illustrates the voltage profile of the IEEE-69 bus network, considering the impact of various distributed generation types in conjunction with EVCSs.

V. CONCLUSIONS

The incorporation of a significant number of electric vehicles (EVs) negatively impacts system performance, resulting in an increase in power losses, a rise in average voltage deviation index (AVDI), a reduction in voltage stability index (VSI), and a decline in the voltage profile. Consequently, different types of distributed generators (DGs) are incorporated with electric vehicle charging stations (EVCS), and it is observed that an increase in the number of DGs yields improved outcomes. This is performed by implementing a novel optimization algorithm, called the Pelican Optimization Algorithm. In here, the multi-objective function, i.e, reduction of power loss, minimization of Average Voltage Deviation Index, and enhancement of Voltage Stability Index, is formulated and optimized using Particle Swarm Optimization (PSO) and Particle Optimized Algorithm (POA), with POA yielding better results than PSO for both the IEEE-33 and IEEE-69 bus systems. From the results, we can conclude that the Type-IIIC DG outperformed the others. Although PSO performs better in certain cases, POA remains consistent across different performance measures

VI. AUTHOR'S CONTRIBUTION

Conceptualization: Swetha Veligaram and Dr. A Lakshmi Devi.
Methodology: Swetha Veligaram and Dr. A Lakshmi Devi.
Investigation: Swetha Veligaram and Dr. A Lakshmi Devi.
Discussion of results: Swetha Veligaram and Dr. A Lakshmi Devi.
Writing – Original Draft: Swetha Veligaram and Dr. A Lakshmi Devi.
Writing – Review and Editing: Swetha Veligaram and Dr. A Lakshmi Devi.
Resources: Swetha Veligaram and Dr. A Lakshmi Devi.
Supervision: Swetha Veligaram and Dr. A Lakshmi Devi.
Approval of the final text: Swetha Veligaram and Dr. A Lakshmi Devi.

VII. ACKNOWLEDGMENTS

The authors would like to express their sincere gratitude to Sri Venkateswara University College of Engineering for providing the necessary guidance and support.

VIII. REFERENCES

[1] Z. Yu, C. Yang, and Q. Wang, “The impact of large-scale EV charging on the real-time operation of distribution systems: A comprehensive review,” arXiv preprint, Jul. 2025.

[2]. B. Singh, A. Pratap, and P. Tiwari, “A review on optimization techniques for electric vehicles planning in distribution networks,” in Proc. 3rd Int. Conf. Adv. Comput. Software Eng., 2021, pp. 81–94.

[3] M. Kumar *et al.*, “A comprehensive review of optimizing multi-energy multi-objective distribution systems with electric vehicle charging stations,” *World Electric Vehicle Journal*, vol. 15, no. 11, 2024.

[4] Murali, V. and Raj, D.B., 2025. Optimizing Electric Vehicle Charging Stations and Distributed Generators in Smart Grids: A Multi-Objective Meta-Heuristic Approach. *IEEE Latin America Transactions*, *23*(11), pp.1022-1035.

[5] H.Pradeepa, T. Ananthapadmanabha, S. Rani D N, C. Bandhavya, Optimal allocation of combined DG and capacitor units for voltage stability enhancement, Procedia Technol. 21 (2015) 216–223, https://doi.org/10.1016/j. protcy.2015.10.091.

[6] V. K. B. Ponnam and K. Swarnasri, “Multi-Objective Optimal Allocation of Electric Vehicle Charging Stations and Distributed Generators in Radial Distribution Systems using Metaheuristic Optimization Algorithms”, *Eng. Technol. Appl. Sci. Res.*, vol. 10, no. 3, pp. 5837–5844, Jun. 2020.

[7] Teng, Jen-Hao. (2003). A direct approach for distribution system load flow solutions. Power Delivery, IEEE Transactions on. 18. 882 - 887. 10.1109/TPWRD.2003.813818.

[8] Altaf, Mishal & Yousif, Muhammad & Ijaz, Haris & Rashid, Mahnoor & Abbas, Nasir & Khan, Muhammad & Waseem, Muhammad & Noman, Ahmed. (2023). PSO-based optimal placement of electric vehicle charging stations in a distribution network in smart grid environment incorporating backward forward sweep method. IET Renewable Power Generation. 18. 3173-3187. 10.1049/rpg2.12916.

[9] Trojovsky, Pavel & Dehghani, Mohammad. (2022). Pelican Optimization Algorithm: A Novel Nature-Inspired Algorithm for Engineering Applications. Sensors. 22. 855. 10.3390/s22030855.

[10] Reddy, S. S. 2016. Determination of Optimal Location and Size of Static VAR Compensator in a Hybrid Wind and Solar Power System. Int. J. Appl. Eng. Res 11 (23): 11494–11500